Graphene Modified Fluorinated Cation-Exchange Membranes for Proton Exchange Membrane Water Electrolysis

Daniela Ion-Ebrasu[a], Bruno G. Pollet[b*], Adnana Spinu-Zaulet[a], Amalia Soare[a], Elena Cacadea[b], Mihai Varlam[a], Simona Caprarescu[c]

[a]National Institute for Cryogenics and Isotopic Technologies ICSI-Rm. Valcea, National Center for Hydrogen & Fuel Cells, Uzinei Str. no. 4, 240050, Ramnicu Valcea, Romania

[b]Department of Energy and Process Engineering, Faculty of Engineering
Norwegian University of Science and Technology (NTNU)
NO-7491 Trondheim, Norway

[c]University Politehnica of Bucharest, Faculty of Applied Chemistry and Materials Sciences, Department of Inorganic Chemistry, Physical Chemistry and Electrochemistry, Bucharest, Romania

*Corresponding author: Daniela Ion-Ebrasu; email: daniela.ebrasu@icsi.ro

Abstract

One of major current technical challenges in proton exchange membrane water electrolysis (PEMWE) is limited proton conductivity. Nowadays, graphene is considered one of the most promising candidates for improving the ionic transport properties, isotopic selectivity and proton conductivity throughout the unique two-dimensional structure. In this paper, we report on the development of graphene modified commercial membranes (Fumapem®) containing different graphene loadings for PEMWE applications. The membranes are characterized by Scanning Electron Microscopy (SEM) and thermo-gravimetrical and differential thermal analysis (TGA-DSC). Properties of composite membranes are investigated, including water uptake and ion-exchange capacity (IEC). In plane four-electrode arrangement is used to determine the proton conductivity of the composite membranes. It is found that composite membranes show an improved behaviour when compared to pristine commercial membranes and graphene loading can improve proton conductivity. In our conditions, the calculated activation energy (E_a) for proton conduction is found to be about 3.80 kJ mol^{-1} for the composite Fumapem®/graphene membrane with 10 mg graphene loading, lower than of the pristine polymer proton exchange membrane.

Keywords: Membrane; Graphene; Fumapem®; Electrolysis; Proton Conductivity

Introduction

In today's world there is a great concern about global warming [1], which can be ascribed to an increase in the carbon dioxide (CO_2) level released into the atmosphere [2,3]. Several initiatives and treaties have been implemented to reduce the level of anthropogenic CO_2 emissions *e.g.* the Paris Agreement, the Kyoto Protocol and the European Commission (March 2011) have launched ambitious plans to reduce the CO_2 emissions to 25% below the 1990 level by 2020. It is assumed that a greater electrification of the society is required, in this context the *Hydrogen Economy* fits in beautifully. To build the hydrogen society, a safe and environmentally friendly way of producing hydrogen is necessary. One way to produce clean hydrogen is through water electrolysis.

The PEM electrolysis technology represents a perfect system adapted to the requests made in the matter of applying renewable energy sources [4]. This is considered, at present time, the most flexible and sustainable solution for storing renewable energy long-term and on different scales, using the energy surplus generated to produce hydrogen, which is afterwards stored and reconverted into electrical/thermal power through various technologies. A PEM electrolyser can operate at high current densities that can reduce the operational costs, especially for systems coupled with very dynamic energy sources such as wind and solar, where sudden spikes in energy input would otherwise result in uncaptured energy. In PEM electrolysis systems, the solid polymer electrolyte membrane selectively conducts the protons that participate in the water-splitting reaction, creating a locally acidic environment in the cell. Solid polymer electrolyte membrane is the "heart" of the electrolyser [4,5]. Nowadays, Nafion® is the common commercial membrane used for this application. The thickness of membrane is generally between 100-200 μm that is considered a compromise among area-specific resistance, low crossover, and mechanical strength

[5]. The main issue is to develop alternative membranes with high proton conductivity, increased mechanical stability to high pressure, and low hydrogen and oxygen crossover.

Moreover, graphene has an exceptionally high surface area to volume ratio as well as high mechanical and thermal properties. These properties of graphene can be utilized for improving the efficiency of PEM electrolysers, thereby reducing costs. Selective ion/molecule transport through graphene is of high interest but is generally thought to require sub-nanometer to nanometer-sized defect structures at which repulsive forces between graphene and permeants are smaller than in pristine graphene and might be tailored to achieve selective transport [6]. Lozada-Hidalgo and co-workers in 2016 reported the equally surprising result of a strong isotopic selectivity in transport of hydrogen ions across graphene, with proton transport favored by a factor of approximately 11 over deuteron transport [7]. The 2017 study from Lozada-Hidalgo and co-workers reported a larger area-normalized graphene proton conductance of approximately 90 mS cm^{-2} [8]. This proton conductance value substantially increased from the earlier work, but it is still well-below the conductance expected for a Nafion® membrane.

The objective of this work is to study graphene modified fluorinated cation-exchange membrane materials as a possible solution to solid polymer electrolyte membrane for PEMWE. The novelty of this approach is to produce composite membranes exhibiting higher thermal stability and proton conductivity via a simple method of graphene spray coating on commercial PEM materials (Fumapem® membrane).

Experimental Methods

Membranes preparation

The graphene modified fluorinated cation-exchange membranes presented in this study were synthesized by graphene uniformly distributed over the surface of commercial 100 µm thick Fumapem® substrate membranes at various graphene loadings. The graphene powder of high conductivity, rich porosity and multi-dimensional electron transport pathway was purchased from Alfa Aesar. Nafion® perfluorinated resin solution containing 5% water and 2-Propanol 99+% was purchased from Alfa Aesar.

Three loadings of graphene nanoplatelets, 5, 10, and 15 mg, were added to 2.6 ml Nafion®/water/isopropanol solution corresponding to 0.19, 0.38, 0.57 w/v % accordingly (Table 1). These mixtures were then ultrasonicated (ultrasonic bath, 80 kHz) for 12 hours in order to form a homogenous solution.

A compressed air spray brush was used to spray the graphene solution over the Fumapem® membrane. A 3.3 × 3.3 cm^2 Fumapem® membrane was cut and dipped for 24 hours in DI water in order to reach equilibrium such that the membrane swells, and then the membrane was left for drying. Once the membrane was dried, the solution was then sprayed over one side of the dry membrane using a compressed nitrogen spray brush at a pressure of 1.5 bar.

Table 1. Modified Fumapem® membranes and graphene loading

Membranes	Graphene loading (mg)	Graphene concentration over one side of the membrane (w/v %)	Support
G1	5	0.19	Fumatech® F-14100
G2	10	0.38	
G3	15	0.57	

SEM characterization

A Sigma VP FEG Carl Zeiss SEM was used for microstructural investigation for both the prepared membranes, and for the graphene nanopelets and commerical Fumapem® membranes. They were mounted as-received on a carbon tape and then analysed in liquid nitrogen atmosphere.

Fourier Transform Infrared Spectroscopy (FTIR)

The infrared characterization was carried out by transmittance and ATR-FTIR methods in the domain of 650-4,000 cm^{-1}, by using a Frontier FT-NIR spectrometer with a diamond ATR accessory.

2.4. Thermogravimetric analysis

Thermogravimetric analysis (TGA) and glass transition (T_g) characterizations by differential scanning calorimetry (DSC) and first derived DSC (DDSC) of the membranes (sample mass: ~10 mg) were carried out using a TGA-DSC – NETZCH STA 449 F5 Jupiter, in the temperature range of 25°C –800°C at a heating rate of 10°C min^{-1} under nitrogen flow.

2.5 Water uptake

The water uptake of the graphene modified Fumapem® composite membranes samples was determined at 25°C and 80°C. Fumapem® membranes were also used for comparison purposes [8,9]. The water uptake was calculated using the following equation:

$$\text{Water uptake} = \frac{W_{wet} - W_{dry}}{W_{dry}} \times 100 \quad (1)$$

where W_{wet} and W_{dry} are the masses of the membranes in wet and dry states, respectively.

2.6 Ionic exchange capacity (IEC)

IEC was determined by a titration method. Cation exchange membrane sample was weighed and then immersed in 1 M HCl (the counter-ion was Cl^-) for 24 hours, then rinsed in deionised water, and finally immersed in 1 M NaCl for 24 hours. The NaCl solution was titrated with 0.01 M NaOH. IEC of the ion exchange membranes was calculated by using equation (2) [10-12]:

$$IEC(mmol g^{-1}) = \frac{Volume_{NaOH} * C_{NaOH}}{M_{dry}} \quad (2)$$

2.7 Proton conductivity and activation energy

Conductivity measurements were performed in the in-plane direction by AC impedance spectroscopy using a 4-point Wanatech Membrane Conductivity Cell (MCC), at 100% RH, soaked in DI water, by passing a current through two outer electrodes and measuring the voltage through the inner electrodes [13,14]. In the 4-electrode configuration, there was virtually no current

flowing at the inner voltage sensing electrodes. Therefore, polarization did not occur. The graphene modified PEM membranes were tested in the temperature range of 25°C-100°C. The resistance (R in Ω) of each sample was determined at the frequency producing the minimum imaginary response. The equation used for the conductivity determination is given in equation (3):

$$\sigma = \frac{L}{R*w*t} \qquad (3)$$

where σ is the conductivity in mS cm^{-1}, R is the *real* part of the impedance in Ω, L is the fixed distance between the two electrodes (3 cm), w is the width of the sample (1.5 cm), and t is the thickness of the membrane in cm. In order to ensure transport of the protons (H^+) through the membranes, the samples were kept in water for 24 hours. The electrochemical impedance (EIS) spectra were recorded at different frequencies from 1 MHz to 0.1 Hz and at a signal amplitude of 100 mV using a Princeton Applied Potentiostat/Galvanostat.

The activation energy E_a (kJ mol^{-1}) required for protons (H^+) transfer through the membranes from one free-site to another was calculated using the following *Arrhenius equation* [12,15].

$$ln\sigma = ln\sigma_0 - \frac{E_a}{RT} \qquad (4)$$

where σ_0 is the pre-exponential factor in mS cm^{-1}, R is the gas constant (8.314 J mol^{-1} K^{-1}), and T is the temperature in K.

Results and Discussion

SEM characterization

SEM images of the top the surface of the *as*-prepared membranes were recorded and compared to the SEM images of the graphene nanoplatelets and Fumapem® membranes. It is clear from Figure 1 that the graphene solution had been distributed uniformly inside the membrane matrix. It can also be seen that the roughness of the composite membranes increased with the graphene loading and the surface was uniform, and no cracks were observed due to the proper interaction of graphene with the Fumapem® membrane.

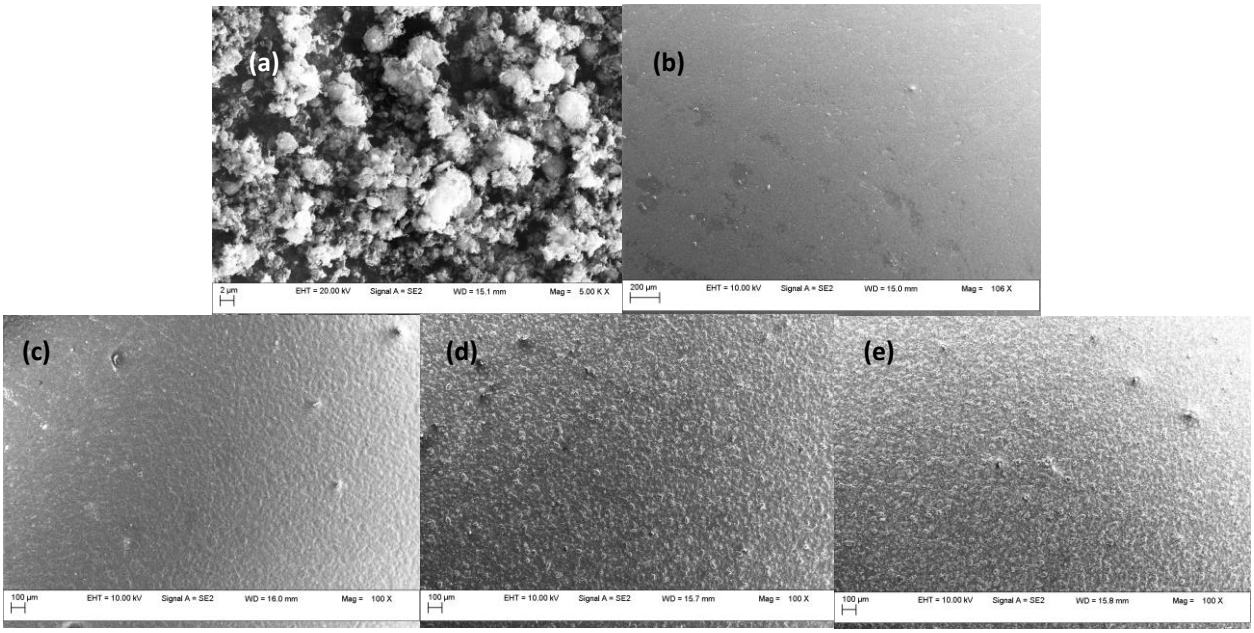

Figure 1. Surface morphology of the G1 (c), G2 (d) and G3 (e) composite membranes, in comparison with graphene (a) and Fumapem® (b) membranes.

Fourier transform infrared spectroscopy (FTIR)

ATR-FTIR analysis was carried out to confirm the presence of graphene in the Fumapem® matrix. Figure 2(a) shows the overlapped spectra of the graphene nanoplatelets, Fumapem® and G1

composite membranes. The spectra of the Fumapem® and the graphene modified composite fluorinated cation-exchange membranes exhibits the characteristic fluorinated CF_2 and CF_3 stretching vibrations situated in the domain of 1,143-1,406 cm^{-1}. The peak at 1,050 cm^{-1} can be associated to S=O symmetric stretching vibrations of the $-SO^{3-}$ ions that are characteristic bands of the sulfonated fluorinated membranes [16,17]. However, in the composite membranes, a decrease and broadening of these peaks can be observed. In comparison with pristine Fumapem® membrane, sample G1 presents an additional peak at 1,705 cm^{-1}, characteristic of the graphene stretching vibration of the C=O group, probably due to the interaction between the graphene and the polymer matrix as well as the formation of the composite membrane [17-19]. Figure 2(b) shows the G1-G3 spectra recorded and compared with pristine Fumapem® in the region of the infrared polymer fingerprint (700 cm^{-1}-2,000 cm^{-1}). Although the ATR-FTIR spectroscopy method cannot quantify the graphene loading, from the spectra presented in Figure 2(b), it can be postulated that Fumapem® functionalization by using graphene nanoplatelets may be possible via simple graphene spray coating.

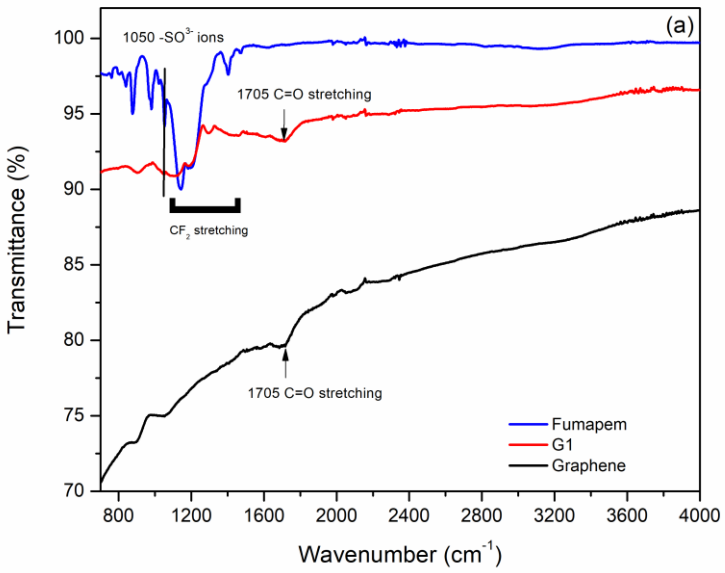

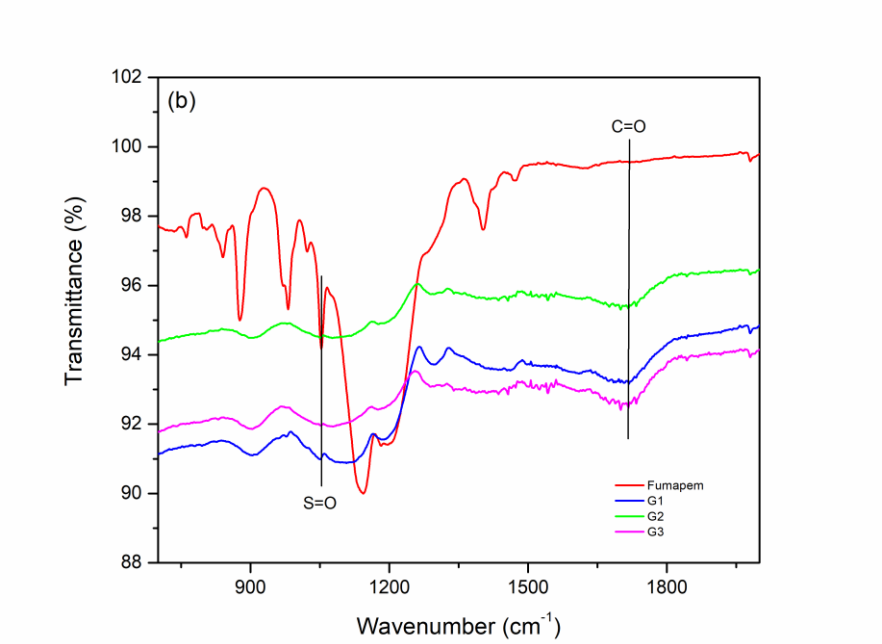

Figure 2. ATR-FTIR spectra of (a) graphene nanoplatelets, Fumapem® and G1 composite membrane; (b) Fumapem®, G1, G2 and G3 in the domain of 700 cm^{-1}-2,000 cm^{-1}

3.3 Thermogravimetric analysis

From the TGA curves presented in Figure 3(a), it can be noticed that both the Fumapem® and composite membranes display three degradation steps: (i) the mass loss assigned to loss of physically and chemically bound water takes place in the temperature range between 318°C-396°C for both the pristine membrane and G1-G3 composites; (ii) the second degradation process is due to sulfonic acid groups decomposition (desulfonation); and (iii) in the temperature range of 450°C–550°C, an additional mass loss step was observed, that can be assigned to the degradation of Fumapem® backbone [12, 20-21]. However, in the first two steps, Fumapem® degrades faster than the composite membranes, indicating a loss of the sulfonic groups at slightly lower temperatures in the case of the Fumapem® membrane, connected with less thermal stability with regard to the G1-G3 samples.

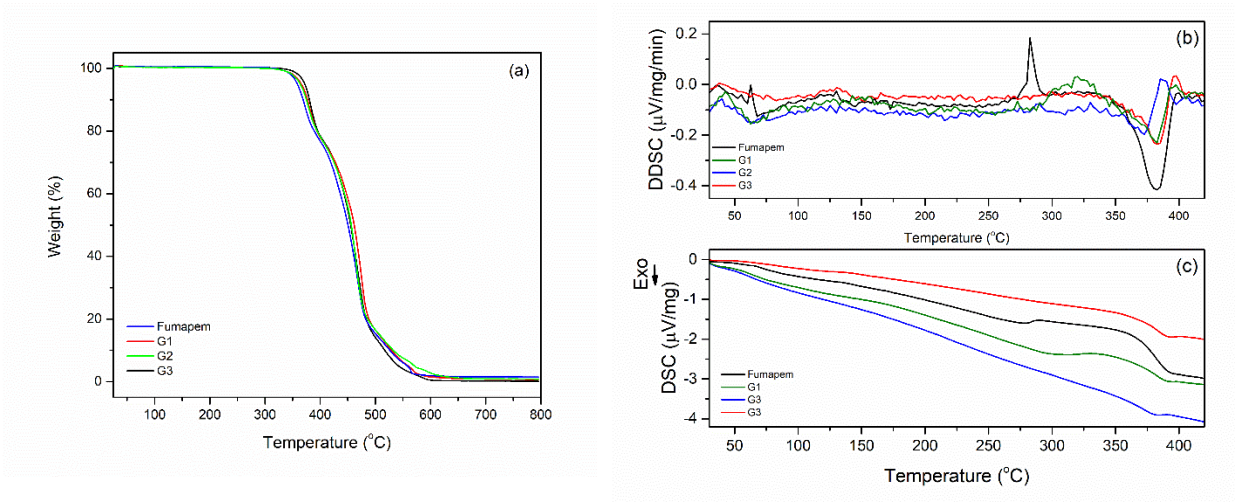

Figure 3. (a) TGA thermograms of Fumapem® and graphene modified membranes G1-G3; (b) DDSC and (c) DSC curves of Fumapem® and G1-G3 membranes.

The glass transition temperature (T_g) was determined from the differential scanning calorimetry (DSC) and first derived DSC (DDSC) of the curves for each membrane. The last one provides more accurate information regarding the membrane structure, considering that the T_g value depends upon the membrane proton conductivity [12,20-22]. The membranes exhibit three endothermic peaks, and one exothermic peak (Fig. 2 (b,c)): (i) the first peak was measured in the temperature range of 35°C-60°C and can be assigned to the relaxation of the fluorocarbon chains [21]; (ii) the broad peak at ca. 130°C correspond to the T_g of the samples; and (iii) the third sharp peak at 282°C corresponds to the Fumapem® sample, and is attributed to the -SO_3 acid groups decomposition. In the case of the G1 membrane, this band exhibits lower intensity, is large and shifted to higher temperatures. However, by increasing the graphene loading, the three peaks' intensity decrease and/or is shifted due to the dipolar interaction between the graphene and the membrane matrix, demonstrating the increase of the sulfonation stability and proton conductivity

due to graphene deposition. It was observed that the exothermic peak at about 380°C corresponds to the membranes' melting point.

3.4 Water uptake and ionic exchange capacity

The water uptake tests performed at 25°C and 80°C showed that graphene/Fumapem® composite membranes absorb more water with respect to the pristine Fumapem®. This is finding is in very good agreement with previous results and confirm that the structure modification of the Fumapem® could be due to the strong interaction of graphene with the fluorinated membrane that leads to increased water content of the composite membranes. A similar trend is also observed when increasing of graphene loading and the ionic exchange capacity (IEC) (Table 2).

Table 2. Water uptake and IEC for Fumapem® and G1-G3 membranes at 25°C and 80°C; proton conductivity and activation energy (E_a)

Membranes	Water uptake (%)		(IEC) (mmol g^{-1})	σ (mS/cm)		E_a (kJ mol^{-1})
	25°C	80°C		25°C	80°C	
Fumapem®	4.21	6.17	0.62	65	91	5.67
G1	5.33	10.94	0.75	75	98	4.61
G2	6.41	14.01	0.82	91	115	3.80
G3	8.22	17.45	0.93	85	109	4.10

3.5 Proton conductivity and activation energy

Proton conductivity of the membranes to a large extent depends upon the amount of water uptake and the ion exchange capacity. The proton conductivity plots are presented in Figure 4(a), and values are summarized in Table 2.

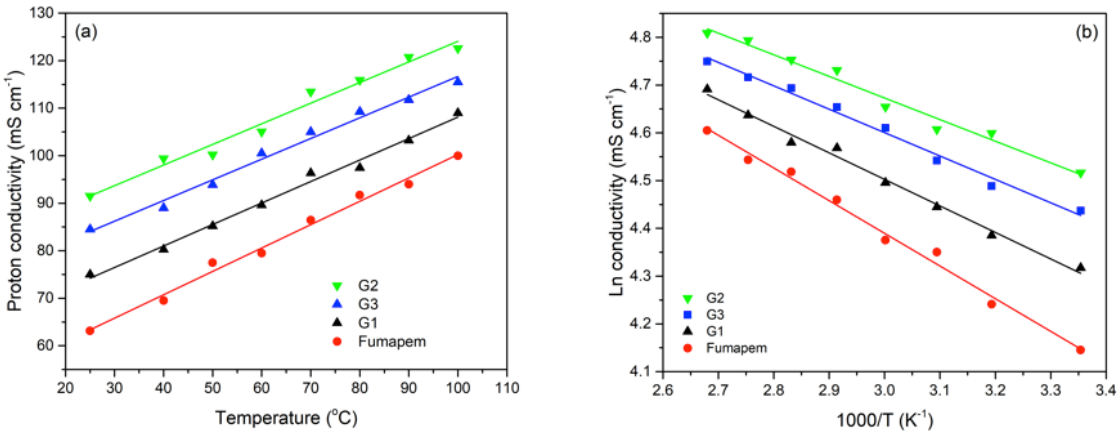

Figure 4. (a) Proton conductivity (a) and, (b) *Arrhenius* plot for the Fumapem® and G1-G3 membranes

Under fully humidified conditions (RH = 100%), the proton conductivity of the composite membranes increases with temperature and graphene content. At a temperature of ca. 80°C, a value of 115 mS cm^{-1} corresponding to 0.38 w/v % of graphene loading can be achieved. For higher graphene loadings, the proton conductivity decreases (membrane G3), which may be due to the excess amount of graphene, hindering and disrupting proton pathway [23,24]. The increased conductivity with the graphene content may be explained by the additional conduction mechanism of protons through nano-confined channels formed between the membrane surface and the graphene layer. According to Figure 4(a), the proton transport can be achieved by the *Grötthus* type proton transport mechanism through hydrogen bonding with water-filled ion pores [13].

From the *Arrhenius* plots (Fig. 4(b)), it was possible to calculate the activation energy (E_a) for Fumapem® and composite membranes (Table 2). It was found that the lowest E_a value (3.8 kJ mol^{-1}) corresponds to membrane G2. The lower E_a of the G2 membrane when compared to the Fumapem® value of 5.67 kJ mol^{-1} suggests that graphene loading can improve the hopping mechanism. Moreover, the decrease of the energy barrier for ion transfer from one free site to another can reduce the energy loss caused by the ionic resistance of the membranes [15]. Therefore, the presence of graphene may help to reach an adequate hydration level and provide additional sites in the composite membranes to maintain proton conductivity and decrease the activation energy.

Conclusions

Composite membranes were successfully developed *via* a simple method of graphene spray coating on Fumapem® membrane surfaces. The structural characterization experiments highlighted that Fumapem® functionalization and composite membranes fabrication was possible. Thermal and electrochemical characterization of the composite membranes showed an improved behaviour when compared to pristine Fumapem® membranes. At 80°C and under 100% RH, a proton conductivity of ca. 115 mS cm^{-1} was achieved at 0.38 w/v % graphene loading on one side of the Fumapem® membrane. Further experimental work is currently being carried out to investigate the behaviour of these graphene/Fumapem® composite membranes under ´real´ electrolyser conditions, paying particular attention to current-voltage measurements.

Acknowledgments

Financial Support: This work was supported by the Romanian National Authority for Scientific Research & Innovation (Contract 117/16.09.2016), and Space Technology and Advanced Research-STAR (Contract 175/20.07.2017).

References

[1] Mann ME, Bradley RS, Hughes MK. Northern hemisphere temperatures during the past millennium: inferences, uncertainties, and limitations. Geophys Res Lett 1999; 26:759-62. http://works.bepress.com/raymond_bradley/17

[2] Cao L, Bala G, Caldeira K, Nemani R, Ban-Weiss G. Importance of carbon dioxide physiological forcing to future climate change. Proc Natl Acad Sci USA2010; 107:9513-8. https://doi.org/10.1073/pnas.0913000107

[3] Princiotta F. Global climate change and the mitigation challenge. J Air and Waste Manag Assoc 2012; 59:1194-211. https://doi.org/10.3155/1047-3289.59.10.1194

[4] Coutanceau C, Baranton S, Audichon T, Hydrogen Electrochemical Production. Cambridge: Academic Press, Ed. Bruno G. Pollet, 2018.

[5] Bessarabov D, Wang H, Li H, Zhao N, PEM Electrolysis for Hydrogen Production, Principles and Applications, 2016 by Taylor & Francis Group, LLC, p. 7.

[6] Zhao YD, Xie YZ, Liu ZK, Wang XS, Chai Y, Yan F. Two-Dimensional Material Membranes: An Emerging Platform for Controllable Mass Transport Applications. Small 2014;10:452142. https://doi.org/10.1002/smll.201401549

[7] Lozada-Hidalgo M, Hu S, Marshall O, Mishchenko A, Grigorenko AN, Dryfe RAW, Radha B, Grigorieva IV, Geim AK. Sieving hydrogen isotopes through two-dimensional crystals. Science 2016;351:68−70. https://doi.org/10.1126/science.aac9726

[8] Lozada-Hidalgo M, Zhang S, Hu S, Esfandiar A, Grigorieva IV, Geim AK. Scalable and efficient separation of hydrogen isotopes using graphene-based electrochemical pumping. Nat Commun 2017;8:1−5, 2017. https://doi.org/10.1038/ncomms15215

[8] Caprarescu S, Radu AL, Purcar V, Ianchis R, Sarbu A, Ghiurea M, Nicolae C, Modrogan C, Vaireanu DI, Périchaud A, Ion Ebrasu D, Adsorbents/ion exchangers-PVA blend membranes: Preparation, characterization and performance for the removal of Zn^{2+} by electrodialysis. Appl Surf Sci 2015;329:65-75. https://doi.org/10.1016/j.apsusc.2014.12.128

[9] Ercelik M, Ozden A, Devrim Y, Colpan CO, Investigation of Nafion based composite membranes on the performance of DMFCs. Int J Hydrogen Energy 2017;42:2658-68. https://doi.org/10.1016/j.ijhydene.2016.06.215

[10] Garcia-Vasquez W, Ghalloussi R, Dammak L, Larchet C, Nikonenko V, Grande D, Structure and properties of heterogeneous and homogeneous ion-exchange membranes subjected to ageing in sodium hypochlorite. J Membr Science 2014;452:100-16. https://doi.org/10.1016/j.memsci.2013.10.035

[11] Ravi Kumar, Chenxi Xu and Keith Scott, Graphite oxide/Nafion composite membranes for polymer electrolyte fuel cells, RSC Advances, 2012, 2, 8777–8782, https://doi.org/10.1039/C2RA20225E

[12] Kim AR, Vinothkannan M, Yoo DJ, Sulfonated fluorinated multi-block copolymer hybrid containing sulfonated(poly ether ether ketone) and graphene oxide: A ternary hybrid membrane

architecture for electrolyte applications in proton exchange membrane fuel cells. J Energy Chem 2018;27:1247–60, https://doi.org/10.1016/j.jechem.2018.02.020

[13] Maldonado L, Perrin J-C, Dillet J, Lottin O, Characterization of polymer electrolyte Nafion membranes: Influence of temperature, heat treatment and drying protocol on sorption and transport properties. J Membr Sci 2012;389:43– 56. https://dx.doi:10.1016/j.memsci.2011.10.014

[14] Sone Y, Ekdunge P, Simonsson D, Proton Conductivily of Nafion 117 as Measured by a Four-Electrode AC Impedance Method. J Electrochem Soc 1996;143(4):1254-9. https://doi.org/10.1149/1.1836625

[15] Jiang Z, Zhao X, Fu Y, Manthiram A, Composite membranes based on sulfonated poly(ether ether ketone) and SDBS-adsorbed graphene oxide for direct methanolfuel cells. J Mater Chem 2012; 22:24862–9. https://doi.org/10.1039/C2JM35571J

[16] J. Ostrowska, A. Narebska, Infrared study of hydration and association of functional groups in perfluorinated Nafion membrane, Part 1. Colloid Polym Sci 1983; 261:93-98. https://doi.org/10.1007/BF01410686.

[17] Thakur VK, Tan EJ, Lin M-F, Lee PS, Poly(vinylidene fluoride)-graft-poly(2-hydroxyethyl methacrylate): a novel material for high energy density capacitors. J Mater Chem 2011;21:3751–9. https://doi.org/10.1039/C0JM02408B

[18] Kumar R, Mamlouk M, Scott K, A Graphite Oxide Paper Polymer Electrolyte for Direct Methanol Fuel Cells. Int. J. of Electrochemistry 2011, Article ID 434186. https://doi.org/10.4061/2011/434186.

[19] Mohamadi S, Preparation and Characterization of PVDF/PMMA/Graphene Polymer Blend Nanocomposites by Using ATR-FTIR Technique, p. 218. https://doi.org/10.5772/36497

[20] Wu, C. M., Xu, T., W. and Yang, W. H. Synthesis and characterizations of new negatively charged organic–inorganic hybrid materials: effect of molecular weight of sol–gel precursor, J. of Solid State Chem. 2004; 177(4–5):1660 – 1666. https://doi.org/10.1016/j.jssc.2003.12.021

[21] Mokhtaruddin SR, Mohamad AB, Loh KS, Kadhum AAH, Thermal properties and conductivity of Nafion-Zirconia composite membrane. Malays J Anal Sci 2016;20(3):670 – 77. DOI: http://dx.doi.org/10.17576/mjas-2016-2003-28

[22] Di Noto V, Piga M, Pace G, Negro E, Lavina S, Dielectric Relaxations and Conductivity Mechanism of Nafion: Studies Based on Broadband Dielectric Spectroscopy. ECS Transactions, 2008;16 (2):1183-93. http://dx.doi.org/10.1149/1.2981960

[23] Paul DK, McCreery R, Karan K, Proton Transport Property in Supported Nafion Nanothin Films by Electrochemical Impedance Spectroscopy. J Electrochem Soc 2014;161(14):F1395-402. http://dx.doi.org/10.1149/2.0571414jes

[24] Parthiban V, Akula S, Peera SG, Islam N, Sahu AK, Proton Conducting Nafion-Sulfonated Graphene Hybrid Membranes for Direct Methanol Fuel Cells with Reduced Methanol Crossover. Energy Fuels 2016;30:725−34. http://dx.doi.org/10.1021/acs.energyfuels.5b02194